# Seismic modeling by demigration

Lúcio T. Santos*, Jörg Schleicher*,
Martin Tygel*, and Peter Hubral‡

## ABSTRACT

Kirchhoff-type, isochron-stack demigration is the natural asymptotic inverse to classical Kirchhoff or diffraction-stack migration. Both stacking operations can be performed in true amplitude by an appropriate selection of weight functions. Isochron-stack demigration is closely related to seismic modeling with the Kirchhoff integral. The principal objective of this paper is to show how demigration can be used to compute synthetic seismograms. The idea is to attach to each reflector in the model an appropriately stretched (i.e., frequency-shifted) spatial wavelet. Its amplitude is proportional to the reflection coefficient, transforming the original reflector model into an artificially constructed true-amplitude, depth-migrated section. The seismic modeling is then realized by a true-amplitude demigration operation applied to this artificially constructed migrated section. A simple but typical synthetic data example indicates that modeling by demigration yields results superior to conventional zero-order ray theory or classical Kirchhoff modeling.

## INTRODUCTION

The Kirchhoff migration integral (see, e.g., Bleistein, 1987; Schleicher et al., 1993; Sun and Gajewski, 1997) is often understood as the approximate inverse operation to forward modeling with the classical Kirchhoff integral (Frazer and Sen, 1985). The Kirchhoff modeling integral is used to propagate a given incident wavefield (e.g., an elementary compressional wave) from the reflector to the receiver point by superimposing Huygens' secondary sources. In the same way, the Kirchhoff migration integral reconstructs the same Huygens' secondary sources along the reflector (in position and strength) from the measured seismic elementary-wavefield reflections at several receiver positions along the seismic line.

As discussed qualitatively by Hubral et al. (1996) and quantitatively by Tygel et al. (1996), there exists an asymptotic inverse to the Kirchhoff migration integral. This inverse has the same structure as the Kirchhoff migration integral. As the latter, it is given by a stacking process that is now applied to the depth-migrated section. To better understand the process, we first recall that the Kirchhoff depth-migrated section is constructed by stacking the original seismic time-domain data along certain stacking surfaces (or curves for 2-D data). These are constructed for a given macrovelocity model without the need to determine (nor identify) the location of the reflection traveltime surfaces in the seismic data. The inverse process can be formulated as a similar stack along related surfaces. These are also constructed for the given macrovelocity model without knowing the location of the reflectors in the migrated data. The stacking surfaces are simply the isochrons, i.e., the surfaces of equal reflection time between a given source and receiver. These isochrons (ellipsoids in the constant-velocity case) are defined by the same traveltimes as the Kirchhoff-type diffraction traveltime surfaces (hyperboloids in the constant-velocity case) that define the stacking surfaces for migration. Thus, all that needs to be known to perform the inverse reflection imaging process by stacking is the same macrovelocity model as used for the Kirchhoff migration. Because of its fundamental similarity to Kirchhoff migration, the inverse to the Kirchhoff migration integral is called Kirchhoff demigration (Whitcombe, 1991, 1994; Kaculini, 1994; Ferber, 1994).

An example of applying the cascade of migration and demigration is a nonlayer-stripping approach for depth-conversion purposes. Whitcombe (1991; 1994) describes how the combination of demigration with single-step ray migration can be used to quickly improve a layered macrovelocity model. Velocity analysis is another important field where demigration has already found a practical application (Ferber, 1994). Demigration can be used to directly compare seismic time sections. All that must be done is to demigrate the migrated sections obtained from different common-offset sections using the original macrovelocity model. Moreover, the processing sequence

of migration and demigration has the potential of being used in data regularization. Seismic reflection data acquired on an irregular grid can be migrated to depth (using a macrovelocity model as accurate as possible) and then demigrated with the same model back into the time-domain data space onto a regular grid. Although expensive, this should provide a very good data interpolation (and even extrapolation) technique because it accounts more correctly for the propagation effects in the reflector overburden. Another class of potential applications lies in least-squares migration (Nemeth et al., 1999; see also references there).

The fact that the familiar Kirchhoff migration integral seems to have two inverse integrals in an approximate sense (i.e., the Kirchhoff modeling integral and Kirchhoff demigration integral) leads inevitably to the question whether the two processes described by these integrals are identical. The answer is that, although closely related, they are different processes. Their close relationship, however, leads to the conclusion that it should be possible to use Kirchhoff demigration to achieve the goals of Kirchhoff forward modeling. In this paper, we elaborate on how this can be done. Duquet et al. (2000) discuss a similar idea, the construction of a new Kirchhoff modeling operator as the transpose of Kirchhoff migration. By means of numerical examples, they show how such a modeling operator can be used to improve the image quality and reduce the cost of least-squares migration.

Although the two integrals describing Kirchhoff forward modeling and Kirchhoff demigration both appear to be inverses to Kirchhoff migration in an asymptotic sense, they do not exactly coincide. Jaramillo and Bleistein (1997) investigate their relationship. They show that both integrals possess the same stationary points (i.e., specular reflection points) and that their integrands are identical at these points. Since the main contributions of both integrals stem from the specular reflection points, their asymptotic evaluation results in the same expression for the reflected wavefield. Thus, we can interpret the demigration integral as a reorganized Kirchhoff modeling integral, which should give very similar results. However, the physical interpretation of this new integral is different. Unlike the Huygens' secondary source contributions in the Kirchhoff integral, it is now the individual Fresnel zone contributions to each primary reflection that are summed by the integration (Schleicher et al., 1997).

So what are the advantages of implementing the new seismic modeling scheme, which we call modeling by demigration, that makes use of the Kirchhoff demigration integral instead of the conventional Kirchhoff modeling integral? There are several advantages.

1)  The actual process of true-amplitude Kirchhoff demigration is so similar to true-amplitude Kirchhoff migration that existing migration programs can be readily modified to include the demigration and the seismic modeling part.
2)  The Green's functions needed for migration and demigration are actually the same. When chaining migration and demigration, the same Green's functions tables can be used.
3)  By its intrinsic structure, modeling by demigration is particularly advantageous when the effects of small structural reservoir changes are to be modeled, as is the case in 4-D or time-lapse imaging. Because the macrovelocity model remains the same, the necessary Green's functions

computations need be carried out only once for a number of modeling studies.
4)  Since demigration is a stacking process, it smoothes the simulated reflection responses (in contrast to, e.g., standard ray theory, which computes arrival times and amplitudes along specular rays only). Thus, there is no need to construct smooth reflectors (e.g., by applying splines) or explicit two-point ray tracing. Modeling by demigration can be applied directly to the conventionally picked reflectors that are usually a sequence of planar reflector elements. This will not damage the simulated reflection response.
5)  The demigration integral constructively sums only contributions from the actual Fresnel zone surrounding each specular reflection point. This fact can be used to restrict the stacking aperture to avoid the summation of unnecessary noise (Schleicher et al., 1997).

The paper is organized as follows. After describing the earth model, we address the difference between modeling and demigration. To prepare the reader for the inclusion of the true-amplitude demigration integral in the new forward-modeling approach (i.e., modeling by demigration), we review the true-amplitude migration integral. Thereafter, we apply the new modeling approach to a simple example, for which the computed synthetic seismograms surpass those obtained by Kirchhoff modeling and ray theory.

## MODELING, MIGRATION, AND DEMIGRATION

Before introducing seismic modeling by demigration as a tool for constructing synthetic seismograms, let us first comment on the basic characteristics of demigration versus forward modeling.

### Basic model assumptions

We assume that primary elementary wave propagation is modeled in a layered, isotropic, inhomogeneous earth model with smoothly curved interfaces (Figure 1). Within the layers, the medium parameters vary smoothly, such that a high-frequency approximation is justified.
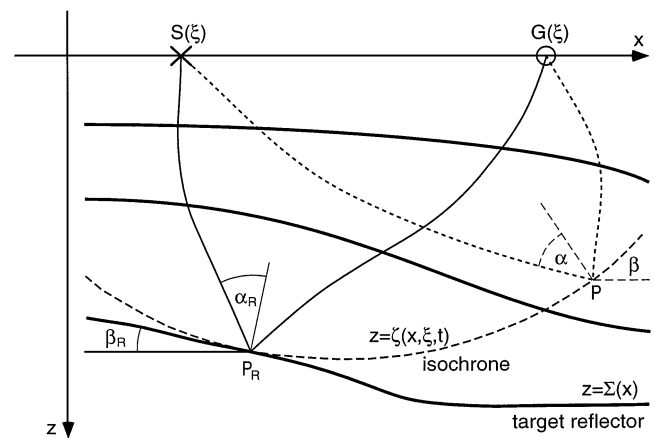
FIG. 1. Inhomogeneous earth model with smooth interfaces. Also shown is one isochron for the indicated source–receiver pair.

To better explain the principles underlying modeling by demigration, we arbitrarily choose one of the many reflecting interfaces as the target reflector. The process described for one reflector and its primary elementary reflection applies simultaneously to all interfaces for which reflection responses are to be modeled.

For simplicity, we refrain from including transmission losses in the following discussions. However, these overburden effects can be appropriately accounted for by including them in the necessary Green's functions computations. This is true for Kirchhoff modeling as well as for Kirchhoff migration and demigration.

### Modeling with the Kirchhoff integral

For a fixed source–receiver pair $(S, G)$ (Table 1), the Kirchhoff forward-modeling integral computes the reflected wavefield as a superposition of primary-reflected wave contributions along all reflecting interfaces under consideration. Since the superposition is a linear process, we restrict the present analysis to a single target reflector $z = \Sigma(\mathbf{x})$. Here, $\mathbf{x}$ is a 2-D vector describing the horizontal coordinates in a global Carte-

### Table 1. Nomenclature

| | |
|---|---|
| $\mathcal{A}$ | Amplitude factor for modeling by demigration |
| $D(\boldsymbol{\xi}, t)$ | Time-domain data |
| $F[t]$ | Analytic source pulse |
| $G$ | Receiver position |
| $ID(\boldsymbol{\xi}, t)$ | Kirchhoff demigrated section |
| $IK(\boldsymbol{\xi}, t)$ | Kirchhoff synthetic section |
| $IM(\mathbf{x}, z)$ | Kirchhoff migrated section |
| $\mathcal{L}$ | 3-D geometrical-spreading factor of the reflection ray from $S$ to $G$ |
| $M(\mathbf{x}, z)$ | Migrated data |
| $P$ | Point with coordinates $(\mathbf{x}, z)$ in depth |
| $P_R$ | Stationary point on the reflector with coordinates $(\mathbf{x}^*, \Sigma(\mathbf{x}^*))$ |
| $P_\Sigma$ | Point on the reflector with coordinates $(\mathbf{x}, \Sigma(\mathbf{x}))$ |
| $\mathcal{P}$ | Prestretch factor for modeling by demigration |
| $\mathcal{R}$ | angle-dependent reflection coefficient at the target reflector |
| $S$ | Source position |
| $\mathcal{S}$ | Migration stretch factor |
| $T$ | Traveltime between two points |
| $t$ | Time coordinate |
| $v_R / \tilde{v}_R$ | Acoustic wave velocity at $P_R$ above/below the reflector |
| $W(\boldsymbol{\xi}, P_\Sigma)$ | Weight function for the Kirchhoff modeling integral |
| $W_D(\mathbf{x}, \boldsymbol{\xi}, t)$ | Weight function for the Kirchhoff demigration integral |
| $W_M(\boldsymbol{\xi}, P)$ | Weight function for the Kirchhoff migration integral |
| $\mathbf{x}$ | Horizontal coordinate (2-D vector) |
| $\mathbf{x}^*$ | Stationary point of both Kirchhoff modeling and Kirchhoff demigration integrals |
| $z$ | Depth coordinate |
| $\alpha_R$ | Reflection angle at $P_R$ |
| $\beta_R$ | Local in-plane reflector dip angle at $P_R$ |
| $\boldsymbol{\xi}$ | Coordinate of the source–receiver pair $(S, G)$ (2-D vector) in the original time section |
| $\boldsymbol{\xi}^*$ | Stationary point of the Kirchhoff migration integral |
| $\rho_R / \tilde{\rho}_R$ | Density at $P_R$ above/below the reflector |
| $\Sigma$ | Reflector surface defined as $z = \Sigma(\mathbf{x})$ |
| $\zeta$ | Isochron surface defined as $z = \zeta(\mathbf{x}, \boldsymbol{\xi}, t)$ |
| $\mathcal{T}(\boldsymbol{\xi})$ | Reflection traveltime from $S(\boldsymbol{\xi})$ to $P_R$ to $G(\boldsymbol{\xi})$ |
| $\tau(\boldsymbol{\xi}, P_\Sigma)$ | Traveltime from $S(\boldsymbol{\xi})$ to $P_\Sigma$ to $G(\boldsymbol{\xi})$ |

sian system. Moreover, we assume the locations of $(S, G)$ not to be independent but to pertain to a certain measurement configuration described by a 2-D parameter vector $\boldsymbol{\xi}$, i.e., $S = S(\boldsymbol{\xi})$ and $G = G(\boldsymbol{\xi})$. Under these circumstances, the Kirchhoff modeling integral can be written in the Kirchhoff approximation as (Frazer and Sen, 1985; Tygel et al., 1994a)

$$IK(\boldsymbol{\xi}, t) = \frac{1}{2\pi} \iint d^2\mathbf{x} \, W(\boldsymbol{\xi}, P_\Sigma) \, \partial_t F[t - \tau(\boldsymbol{\xi}, P)]|_{z=\Sigma(\mathbf{x})}, \tag{1}$$

where $IK(\boldsymbol{\xi}, t)$ denotes the modeled synthetic seismogram and $z = \Sigma(\mathbf{x})$ is the reflector that defines the integration surface. Also $P = (\mathbf{x}, z)$ is an arbitrary point in depth, and $P_\Sigma = P|_{z=\Sigma(\mathbf{x})} = (\mathbf{x}, \Sigma(\mathbf{x}))$. Moreover, $W(\boldsymbol{\xi}, P_\Sigma)$ is a kernel or weight function consisting of an obliquity factor, the specular plane-wave reflection coefficient of the incident wave at the reflector, and two Green's function amplitudes. The latter pertain to the wave propagation along the two paths from the source $S(\boldsymbol{\xi})$ to the point $P_\Sigma = (\mathbf{x}, z = \Sigma(\mathbf{x}))$ on the reflector and from there to the receiver $G(\boldsymbol{\xi})$ (see Figure 1). Moreover, $F[t]$ is the analytic pulse chosen to represent the source signature, and

$$\tau(\boldsymbol{\xi}, P_\Sigma) = T(S(\boldsymbol{\xi}), P_\Sigma) + T(G(\boldsymbol{\xi}), P_\Sigma) \tag{2}$$

is the sum of traveltimes along the two paths of propagation $SP_\Sigma$ and $GP_\Sigma$, where $S(\boldsymbol{\xi})$ and $G(\boldsymbol{\xi})$ are fixed and $P_\Sigma$ varies along the reflector. In the case of many reflectors, an integral of the type of equation (1) must be evaluated along each of them.

Integral (1) can be asymptotically evaluated as the sum of contributions of its stationary points (Bleistein, 1984). These are the specular reflection points $P_R(\boldsymbol{\xi}) = P_\Sigma|_{\mathbf{x}=\mathbf{x}^*(\boldsymbol{\xi})}$ on the reflector that pertain to the given source–receiver pair $S(\boldsymbol{\xi})$ and $G(\boldsymbol{\xi})$ specified by $\boldsymbol{\xi}$. Assuming, for simplicity, a unique specular reflection $P_R$ (see Figure 1), the asymptotic evaluation yields the zero-order ray approximation

$$IK(\boldsymbol{\xi}, t) \approx \frac{\mathcal{R}(\boldsymbol{\xi})}{\mathcal{L}(\boldsymbol{\xi})} F[t - \mathcal{T}(\boldsymbol{\xi})], \tag{3}$$

where $\mathcal{R}(\boldsymbol{\xi})$ is the reflection coefficient, $\mathcal{L}(\boldsymbol{\xi})$ is the geometrical spreading factor, and $\mathcal{T}(\boldsymbol{\xi}) = \tau(\boldsymbol{\xi}, P_R)$ is the reflection traveltime. All of these quantities pertain to the specular ray denoted by $SP_RG$. For many reflectors, the modeled synthetic seismogram section will be a superposition of seismic reflections of type (3).

We stress again that here, as well as in the following, additional amplitude effects such as transmission losses at overburden interfaces and absorption are neglected for simplicity. These effects can be included independently in each of the methods to be discussed in this paper.

### True-amplitude migration

Kirchhoff migration is based on the idea of stacking the time-domain data in such a way that any reflections possibly pertaining to a certain, arbitrarily chosen depth point $P = (\mathbf{x}, z)$ are summed together. Kirchhoff migration can be represented in the form of the following stacking integral (Bleistein, 1987; Schleicher et al., 1993):

$$IM(\mathbf{x}, z) = -\frac{1}{2\pi} \iint d^2\boldsymbol{\xi} \, W_M(\boldsymbol{\xi}, P) \, \partial_t D(\boldsymbol{\xi}, t)|_{t=\tau(\boldsymbol{\xi}, P)}, \tag{4}$$

where $IM(\mathbf{x}, z)$ denotes the depth-migrated section, $W_M(\boldsymbol{\xi}, P)$ is the true-amplitude weight function, and $D(\boldsymbol{\xi}, t)$ are the seismic time-domain data to be migrated. In correspondence to equation (2),

$$\tau(\boldsymbol{\xi}, P) = T(S(\boldsymbol{\xi}), P) + T(G(\boldsymbol{\xi}), P) \qquad (5)$$

is the sum of traveltimes along the two paths of propagation $SP$ and $PG$. Now, however, $P$ is an arbitrary, fixed point in the subsurface, and $S(\boldsymbol{\xi})$ and $G(\boldsymbol{\xi})$ vary along the measurement surface (see Figure 1).

Like the Kirchhoff integral (1), integral (4) can also be evaluated asymptotically. For all primary reflections described in the zero-order ray approximation of equation (3), an evaluation of the Kirchhoff migration integral (4) in the vicinity of a specular reflection point $P_R$ on an (unknown) reflector $z = \Sigma(\mathbf{x})$ (see Figure 1) yields the reflector image (Tygel et al., 1996)

$$IM(\mathbf{x}, z) \approx \mathcal{R}(\boldsymbol{\xi}^*)F[\mathcal{S}(\mathbf{x})(z - \Sigma(\mathbf{x}))]. \qquad (6)$$

In other words, Kirchhoff migration (4) reconstructs the source wavelet in the vicinity of point $P_R$ on the reflector $z = \Sigma(\mathbf{x})$. The point $P_R$ determines the stationary point $\boldsymbol{\xi}^*$ of integral (4), which in turn defines the specularly reflected ray $S(\boldsymbol{\xi}^*)P_R G(\boldsymbol{\xi}^*)$. The peak amplitude of the migrated pulse is given by the reflection coefficient $\mathcal{R}(\boldsymbol{\xi}^*)$. Thus, Kirchhoff migration (4) frees the primary reflection event $D(\boldsymbol{\xi}^*, t)$ from its geometrical-spreading loss but stretches the wavelet by the factor (Tygel et al., 1994b)

$$\mathcal{S}(\mathbf{x}) = \frac{2 \cos \alpha_R \cos \beta_R}{v_R}, \qquad (7)$$

where $\alpha_R$ is the reflection angle, $\beta_R$ is the local (in-plane) reflector dip angle, and $v_R$ is the velocity at the specular reflection point $P_R$. Further from the reflector, the stack (4) yields a negligible value.

The main advantage of Kirchhoff migration (4) is that neither the primary reflections nor the reflector positions need to be identified. The same integration (or stacking) process is applied independently of the number and locations of the primary reflection events and reflecting interfaces. All reflector images will be represented by an expression of type (6).

Although often referred to as such, migration cannot be considered an inverse process to modeling—not even in an asymptotic sense. In fact, migration is the adjoint operation to modeling (Berkhout, 1982). Migration is not designed to reconstruct the original earth model but to locate its reflecting interfaces and provide angle-dependent reflection coefficients as amplitude measures in the migrated section. Recovery of the physical parameters needed as the input to forward modeling is done by an additional process called inversion. Inversion is usually applied in a chain with migration, referred to as migration/inversion (see Beydoun and Mendes, 1989). Without the inversion step, migrated data cannot be used as an input to modeling. They can, however, be used directly as an input to demigration.

**True-amplitude demigration**

Similar to the arguments that lead to the Kirchhoff migration formula, a structurally equivalent integral can be set up for its inverse operation (Hubral et al., 1996; Tygel et al., 1996). The idea is to stack along a certain surface in the depth-migrated data volume in such a way that any migrated events that possibly pertain to a certain, fixed point $(\boldsymbol{\xi}, t)$ in the demigrated section are summed together. This process is represented by the Kirchhoff demigration integral

$$ID(\boldsymbol{\xi}, t) = \frac{1}{2\pi} \iint d^2\mathbf{x} \, W_D(\mathbf{x}, \boldsymbol{\xi}, t) \, \partial_z M(\mathbf{x}, z)|_{z=\zeta(\mathbf{x},\boldsymbol{\xi},t)}, \qquad (8)$$

where $ID(\boldsymbol{\xi}, t)$ denotes the demigrated data, $W_D(\mathbf{x}, \boldsymbol{\xi}, t)$ is again a true-amplitude weight function to treat amplitudes correctly, and $M(\mathbf{x}, z)$ is the migrated data to be demigrated. These are obtained from a previous migration, although not necessarily from a Kirchhoff migration. The stacking surface, $z = \zeta(\mathbf{x}, \boldsymbol{\xi}, t)$, is implicitly given by

$$t = \tau(\boldsymbol{\xi}, \mathbf{x}, z = \zeta(\mathbf{x}, \boldsymbol{\xi}, t)) = T(S(\boldsymbol{\xi}), P) + T(G(\boldsymbol{\xi}), P), \qquad (9)$$

i.e., by the very same sum of traveltimes (2) as used in Kirchhoff forward modeling (1) and Kirchhoff migration (4). As in Kirchhoff modeling, $S(\boldsymbol{\xi})$ and $G(\boldsymbol{\xi})$ are the fixed source and receiver points specified by the configuration parameter $\boldsymbol{\xi}$. Here, however, $P = (\mathbf{x}, z)$ does not vary along the reflector $z = \Sigma(\mathbf{x})$ but along the surface $z = \zeta(\mathbf{x}, \boldsymbol{\xi}, t)$ This is constructed in the given macrovelocity model according to equation (9) under the condition that $t$ is constant. In other words, $z = \zeta(\mathbf{x}, \boldsymbol{\xi}, t)$ describes the surface of equal reflection time or isochron pertaining to the pair $S$ and $G$ and a given time $t$ (see Figure 1). This isochron plays the same role in Kirchhoff demigration (8) as the diffraction-time surface plays in Kirchhoff migration (4). In both cases, the stacks sum all contributions that come from the Fresnel zones surrounding the specular reflection points.

Assume that the original time-domain data were migrated using some migration scheme whose amplitude and stretching properties are unknown. The resulting reflector images can still be represented, correspondingly to equation (6), by an expression of the type

$$M(\mathbf{x}, z) = \mathcal{A}(\mathbf{x})F[\mathcal{P}(\mathbf{x})(z - \Sigma(\mathbf{x}))], \qquad (10)$$

where $\mathcal{A}$ describes the amplitude of the migrated reflections and $\mathcal{P}$ is a certain prestretch factor produced by the migration operation. Applying the demigration integral (8) to the reflector image in equation (10) yields, after asymptotic evaluation as before,

$$ID(\boldsymbol{\xi}, t) \approx \frac{\mathcal{A}(\mathbf{x}^*)}{\mathcal{L}(\boldsymbol{\xi})} F[\mathcal{S}(\mathbf{x}^*)^{-1}\mathcal{P}(\mathbf{x}^*)(t - \mathcal{T}(\boldsymbol{\xi}))], \qquad (11)$$

where $\mathbf{x}^* = \mathbf{x}^*(\boldsymbol{\xi})$ is the stationary point describing the specular reflection ray $S(\boldsymbol{\xi})P_R G(\boldsymbol{\xi})$. The amplitude after true-amplitude demigration becomes the ratio between the original amplitude $\mathcal{A}(\mathbf{x}^*)$ of the input migrated data, evaluated at the stationary point, and the geometrical spreading factor $\mathcal{L}(\boldsymbol{\xi})$ along the reflection ray $S(\boldsymbol{\xi})P_R G(\boldsymbol{\xi})$. This is in contrast with true-amplitude migration, where the geometrical spreading factor is removed from the input amplitudes [see equation (6)]. We recall that $\mathcal{T}(\boldsymbol{\xi}) = \tau(\boldsymbol{\xi}, P_R)$ is the reflection traveltime along ray $S(\boldsymbol{\xi})P_R G(\boldsymbol{\xi})$ and that $P_R = P_\Sigma|_{\mathbf{x}=\mathbf{x}^*}$.

Tygel et al. (1995) show that the pulse stretch caused by demigration is the inverse to migration stretch given in equation (7). In other words, Kirchhoff demigration unstretches

the seismic signal by the same factor $\mathcal{S}$ by which Kirchhoff migration stretches it. Hence, after Kirchhoff migration and demigration, no overall stretch factor remains in formula (11).

Like Kirchhoff migration, Kirchhoff demigration does not depend on the number and locations of primary reflections or reflector images. The demigrated section is thus a superposition of all demigrated reflector images (i.e., primary reflection events) of the type of equation (11).

The demigration result $ID(\mathbf{x}, t)$ is designed to closely reconstruct the original field data, $ID(\boldsymbol{\xi}, t) \approx D(\boldsymbol{\xi}, t)$, from its migrated section. Thus, Kirchhoff demigration (8) can be conceived as an (asymptotic) inverse to Kirchhoff migration (4). Motivated by the work of Tygel et al. (1996), Jaramillo and Bleistein (1997) show that the Kirchhoff modeling and demigration integrals (1) and (8) are asymptotically equivalent to each other. This means their leading-order, ray-theory contributions coincide.

### MODELING USING DEMIGRATION

After having stated the similarities and differences between modeling and demigration, let us address the basic question of this paper: How can we use the true-amplitude demigration integral for seismic modeling purposes, and what do we gain from this? For each given subsurface reflector, we must appropriately simulate its corresponding true-amplitude, depth-migrated reflector image as if obtained from a Kirchhoff migration applied to the primary reflection to be modeled. In other words, given the source and receiver positions $S(\boldsymbol{\xi})$ and $G(\boldsymbol{\xi})$, respectively, as well as the reflector $z = \Sigma(\mathbf{x})$ within the velocity model and the analytic source signal $F[t]$, we must artificially construct the true-amplitude reflector image using the expression

$$M(\mathbf{x}, z) = \mathcal{A}(\mathbf{x}) F[\mathcal{P}(\mathbf{x})(z - \Sigma(\mathbf{x}))]. \tag{12}$$

We may say that this is obtained by placing the correctly scaled and stretched source pulse $F[t]$ along the reflector. Here, the amplitude factor $\mathcal{A}(\mathbf{x})$ and the prestretch factor $\mathcal{P}(\mathbf{x})$ have yet to be chosen in such a way that, at the stationary point $\mathbf{x}^* = \mathbf{x}^*(\boldsymbol{\xi})$, they match the correct (plane-wave) reflection coefficient $\mathcal{R}(\boldsymbol{\xi})$ and the correct pulse stretch factor $\mathcal{S}(\mathbf{x}^*(\boldsymbol{\xi}))$, respectively:

$$\mathcal{A}(\mathbf{x}^*) \approx \mathcal{R}(\boldsymbol{\xi}) \quad \text{and} \quad \mathcal{P}(\mathbf{x}^*) \approx \mathcal{S}(\mathbf{x}^*). \tag{13}$$

This construction of an artificial migrated section is the inverse operation to inversion.

A natural choice for $\mathcal{A}$ and $\mathcal{P}$ is to use the actual functions $\mathcal{R}$ and $\mathcal{S}$ of Kirchhoff migration. Unfortunately, this might be difficult because these functions can be obtained only after the specular reflection rays are determined. However, any other pair of smooth functions $\mathcal{A}(\mathbf{x})$ and $\mathcal{P}(\mathbf{x})$ that satisfy conditions (13) at the stationary point will also work. This allows us to use the stationary values of the two functions directly without computing them for other, more distant reflector points.

We now apply the demigration integral (8) to an artificial migrated section containing a superposition of reflector images of the type of equation (12). Amplitude $\mathcal{A}$ and prestretch factor $\mathcal{P}$ are chosen to satisfy equations (13). This leads correspondingly to equation (11), a demigrated or synthetic seismogram

section where all specular primary reflections are of the type

$$ID(\boldsymbol{\xi}, t) \approx \frac{\mathcal{R}(\boldsymbol{\xi})}{\mathcal{L}(\boldsymbol{\xi})} F[t - \mathcal{T}(\boldsymbol{\xi})]. \tag{14}$$

Comparison to equation (3) shows that this is exactly the result of zero-order ray theory or of the asymptotic evaluation of the Kirchhoff modeling integral (1). In other words, the synthetic time section obtained by demigration of this artificially constructed depth-migrated section will be equivalent to the one directly obtained as a result of conventional Kirchhoff forward modeling applied to the given earth model. In addition to the correctly modeled specular reflections [equation (14)], modeling by demigration also provides good estimates of nonspecular events like diffractions or the wavefield near a caustic, as shown below in a numerical example.

### Implementational aspects

Tables of Green's functions from all source and receiver points to all subsurface points within a target region are computed. These provide information about the isochron stacking surfaces and the necessary weight functions along them. However, modeling by demigration includes an additional step: construction of the true-amplitude reflector images in an artificial migrated section, or the inverse operation to inversion. This section discusses how this part of the modeling process can be realized.

*Zero offset.*—For zero-offset modeling, the idea of modeling by demigration can be applied directly. All necessary quantities to construct the migrated image for each reflector are physical parameters directly available from the a priori specified earth model. For any arbitrary zero-offset reflection, the stretch factor at the stationary point on the reflector is given by (Tygel et al., 1994b)

$$\mathcal{S}(\mathbf{x}^*) = \frac{2 \cos \beta_R}{v_R} \tag{15}$$

and the normal-incidence reflection coefficient is given by

$$\mathcal{R}(\boldsymbol{\xi}) = \frac{\tilde{\rho}_R \tilde{v}_R - \rho_R v_R}{\tilde{\rho}_R \tilde{v}_R + \rho_R v_R}. \tag{16}$$

Here, $\beta_R$ is the local reflector dip, and $v_R$, $\tilde{v}_R$ and $\rho_R$, $\tilde{\rho}_R$ are the velocities and densities above and below the considered target reflector at the reflection point. Therefore, $\mathcal{S}$ and $\mathcal{R}$ can be directly computed for any given reflector point. Since all quantities are readily available from the specified earth model, the construction of the artificial migrated section with true-amplitude reflector images of type (12) presents no problem.

*Finite offset.*—For nonzero offsets, modeling by demigration needs a little more effort. Before being attached to the reflectors to construct the artificial migrated section, the wavelet must be multiplied with an amplitude factor $\mathcal{A}$ and stretched by a factor $\mathcal{P}$ satisfying conditions (13). Demigration will then unstretch the spatial wavelets of the reflector image of equation (12) because it is the inverse process to migration. Therefore, the primary-reflection pulses in the resulting synthetic-seismogram section, as given in equation (14), become correct and do not suffer from any stretch.

In this case, the computational problem with equations (13) is that the stretch factor as well as the reflection coefficient

at the specular reflection point depend on the reflection angle $\alpha_R$ of the specular reflected ray between $S(\xi)$ and $G(\xi)$ (see again Figure 1). This means that for each different source–receiver pair in the considered measurement configuration, a differently scaled and stretched wavelet is to be used because the reflection angle differs. However, this angle is not available without previously determining the reflection ray between $S(\xi)$ and $G(\xi)$. Therefore, two-point ray tracing seems necessary to construct the artificial migrated section.

Fortunately, the artificial migrated section need not be constructed explicitly but only implicitly during the demigration procedure. Thus, a prior two-point ray tracing is not necessary. If an explicit construction of the artificial migrated section were desired, one would have to determine first the correct angle-dependent plane-wave reflection coefficient and the stretch factor (7) for each reflection point $P_R$ on the reflector (see Figure 1) by a previous ray tracing. This has been done in the numerical section of this paper for didactic reasons only. However, the actual modeling can be (and has been) done without the explicit use of this artificial section, which is important for efficiency.

The basic observation is that for each primary reflection to be modeled, equations (13) must be satisfied at the stationary point only, i.e., at the specular reflection point $P_R$ in Figure 1. Thus, the specular reflection angle $\alpha_R$, which is the crucial and problematic quantity in the process, can be replaced at each potential reflection point $P$ on the isochron by the half-angle $\alpha$ between the ray segments from the source $S(\xi)$ and the receiver $G(\xi)$ to this point. If a certain depth point on the isochron is an actual specular reflection point $P_R$ for the considered source–receiver pair $S(\xi), G(\xi)$, then this half-angle is equal to the specular reflection angle $\alpha_R$. Therefore, conditions (13) are satisfied. Of course, the contributions from other reflector points that are not specular reflection points for the considered source–receiver pair are altered by this substitution. However, to the leading asymptotic order, the resulting alterations in the stacking sum are negligible. The computation of the half-angle $\alpha$ requires no additional effort since all required Green's function computations must be carried out in any case to determine the isochron stacking surfaces and weight functions. In this way, the pulse-stretch factor and the reflection coefficient can be determined and used implicitly during the demigration process (8).

*Approximate solution.*—If one insists on the explicit construction of the artificial migrated section as the first step, the problem of finding the unknown specular reflection angle $\alpha_R$ can still be avoided using one of the following approximations, either assuming (1) small offsets such that the reflection coefficients and the stretch factors can be replaced by the corresponding quantities for zero offset given in equations (15) and (16) or assuming (2) a weak contrast at the reflector such that the reflection coefficient can be replaced by a linearized scattering coefficient. If seismic reflection events with correct first-arrival traveltimes but incorrect pulses are acceptable, the stretch factor can even be omitted. In other words, the reflector images in the artificial migrated section can then be represented in the form

$$M(\mathbf{x}, z) = \mathcal{A}(\mathbf{x})F[z - \Sigma(\mathbf{x})], \quad (17)$$

with $\mathcal{A}$ being some scattering coefficient, e.g., according to the Born approximation. Application of the true-amplitude demigration stack [equation (8)] to the reflector image [equation (17)] will then result in the seismic reflection response

$$ID(\xi, t) \approx \frac{\mathcal{A}(\mathbf{x}^*(\xi))}{\mathcal{L}(\xi)} F[\mathcal{S}(\mathbf{x}^*(\xi))^{-1}(t - \mathcal{T}(\xi))], \quad (18)$$

the traveltimes of which are correct within the validity limits of zero-order ray theory. The amplitudes, however, are correct within the limits of the considered approximation only.

## NUMERICAL EXAMPLE

To illustrate the modeling by demigration method, we consider the simple one-reflector earth model depicted in Figure 2. For computational simplicity, we choose a 2.5-D situation, which means that 3-D amplitude effects of in-plane propagation are correctly considered in a 2-D medium, i.e., one that does not vary in the out-of-plane direction. The velocities in the half-spaces above and below the reflector are $v_1 = 2500$ m/s and $v_2 = 3000$ m/s, respectively. The density is constant and equal to unity. For this model, we simulate a common-offset experiment with a half-offset of $h = 500$ m. The ray family for the experiment is also shown in Figure 2. A particular reason for choosing this model is the presence of a caustic clearly revealed in the figure.

In Figure 3, we see the artificially constructed migrated reflector image obtained from the model parameters. As mentioned before, this image is depicted here for didactic reasons only and is never explicitly calculated in the actual modeling by demigration process. Together with the artificial migrated image, five isochrons for a certain fixed source–receiver pair and five values of the traveltime are depicted. Along these and many other isochrons, the amplitudes found in the artificial migrated section are stacked like in a Kirchhoff migration. The resulting stack value is placed in the demigrated section into the point determined by the midpoint coordinate of the source–receiver pair and the fixed traveltime defining the isochron. Note that one of the shown isochrons passes through the wavelet attached to the reflector. The true-amplitude stack along this isochron and others in its vicinity will yield the correct amplitude of the corresponding primary reflection event. Stacks along other isochrons away from the reflector image
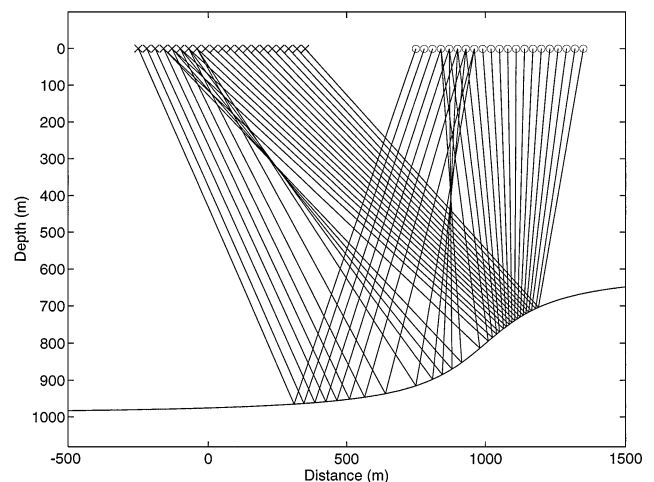


FIG. 2. One-layer model for the numerical experiment.

will yield a negligible value. Figure 3 also indicates the Fresnel zone on the reflector, which depends on the source–receiver pair. In fact, the Fresnel zone determines the wavefield contributions to the primary common-offset reflection. On the other hand, the Fresnel zone of a certain primary reflection is also the part of the reflector where its image contributes to the isochron stack, i.e., where the isochron cuts the spatial wavelets attached to the reflector (Schleicher et al., 1997).

The common-offset section resulting from modeling by demigration has been compared in Figure 4 with the corresponding sections obtained by conventional seismic modeling schemes. Figure 4a shows the synthetic common-offset seismogram section as obtained by classic zero-order ray theory; Figure 4b contains the corresponding section resulting from Kirchhoff forward modeling with integral (1). Figure 4c shows the new modeling by demigration result. In both integration techniques the aperture was chosen large enough to avoid boundary effects. As expected, we observe most fundamental differences between the zero-order ray-synthetic seismograms (Figure 4a) and the ones obtained by both summation processes. As a main feature, the diffracted events, i.e., the caustic tails in the bow-tie structure, are not present in the former. This is because standard ray theory only accounts for specular reflections and cannot handle nonspecular events. In this respect modeling by demigration is more accurate than zero-order ray theory because it includes diffracted-wave contributions as does Kirchhoff forward modeling. This has to be so because, corresponding to Kirchhoff migration, demigration also sums all possible contributions to a given point in the time section to be constructed. It is hard to see any differences between the Kirchhoff synthetic seismogram section and the one obtained from modeling by demigration.

A closer inspection of the seismic forward modeling results is provided in Figure 5, where specific single traces are compared. Figure 5a shows the very first trace of the three seismograms of Figure 4 at the midpoint position of 250 m. We clearly see that, for the specular reflection event, modeling by demigration (solid line) yields practically the same pulse as standard zero-order ray theory (dotted line) and Kirchhoff forward modeling (dashed line). The diffracted event that arrives later is quite
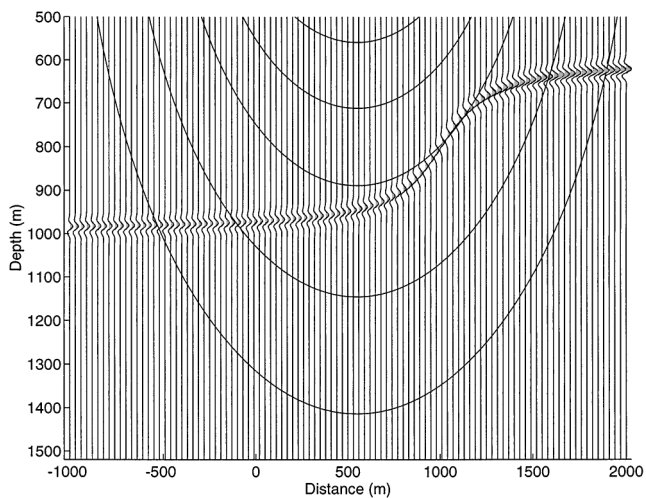


FIG. 3. Artificial migrated section constructed from the model parameters shown in Figure 2.
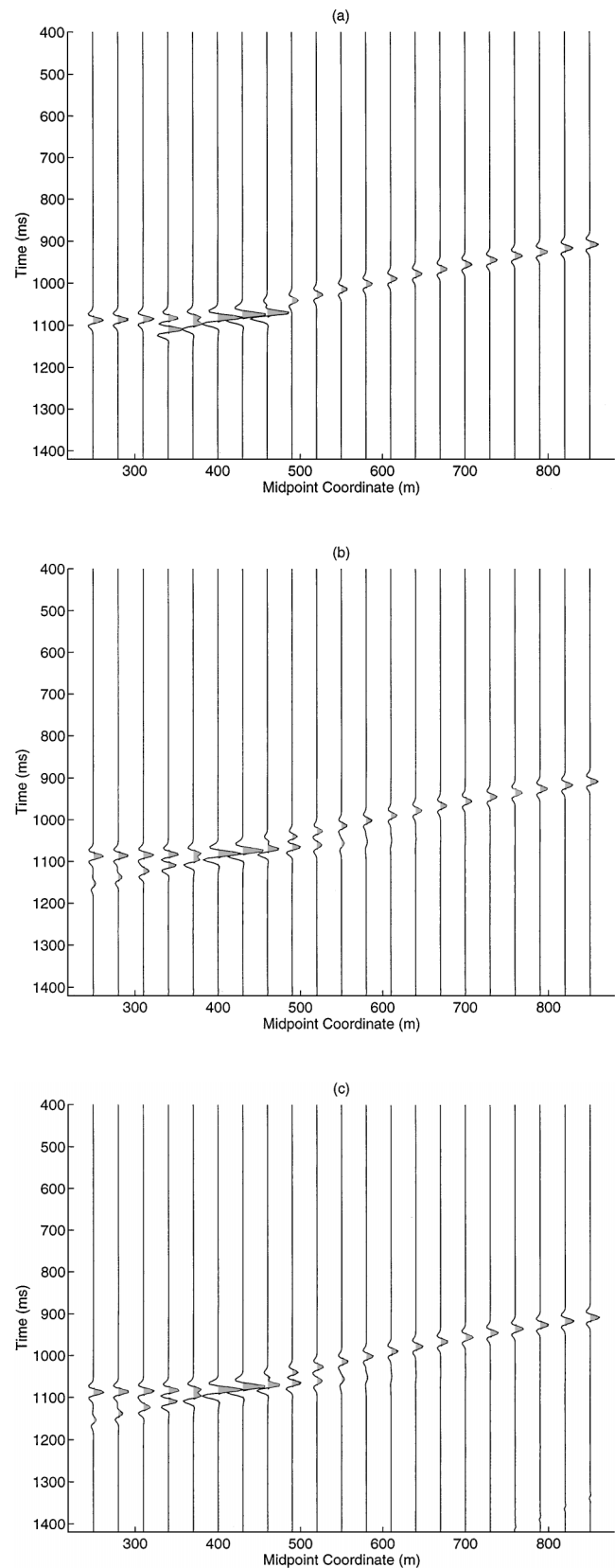


FIG. 4. (a) Modeled common-offset section as a result of zero-order ray theory. (b) Modeled common-offset section as a result of the Kirchhoff integral. (c) Modeled common-offset section as a result of modeling by demigration.

similar to the one obtained from Kirchhoff modeling. This event is not present in the ray-theoretical seismogram trace. However, a third, erroneous event is present in the Kirchhoff modeling trace only. This event arises as a consequence of the Kirchhoff approximation. By studying a planar reflector, for which an analytical solution in integral form is known (Tygel and Hubral, 1987), we can see that the Kirchhoff approximation introduces an additional singularity into the Kirchhoff integral solution that is not present in the analytical solution. This additional singularity does not appear in the Kirchhoff demigration integral. Consequently, the spurious event is not produced by demigration modeling, even though the spatial sampling and apertures for both summations were chosen to be identical and the same approximation for the involved Green's functions are being made.

Figure 5b shows the computation results of the three algorithms for the seismic trace at midpoint position 340 m, that is, the fourth trace of Figure 4. As is clearly visible in Figure 4, this trace contains a caustic event. The three methods produce

almost identical pulses for the first (specular) reflection, the rays of which pass fairly far from the caustic. The second event in that trace consists of an overlap of two (also specular) reflections that have passed through the caustic. The modeling by demigration result and the result from Kirchhoff modeling do not show significant differences. The amplitudes of the caustic events differ slightly. However, with no 3-D finite-difference code available, we do not have a criterion for which is a better approximation of the correct amplitude. Note the wrong large amplitudes provided by ray theory for this caustic situation. This is because ray theory overestimates amplitudes when the receiver is too close to a caustic.

Figure 5c depicts the results of the three methods for constructing the trace at 430 m, i.e., the seventh trace of Figure 4. This trace is interesting because it is exactly in the center of the bow-tie structure, where there is an overlap among all three specularly reflected pulses. Of the three corresponding reflected rays, two pass through a caustic, whereas the third one does not. Ray amplitudes should be correct here because the receiver position is sufficiently far away from the caustic location. In this case modeling by demigration seems to give a better result than Kirchhoff modeling. The pulse obtained by demigration modeling fits the ray-traced pulse quite well, but there is a certain amplitude loss in the Kirchhoff result. Figure 5d confirms this observation. It depicts the seismic trace from the very left of the model, i.e., with a midpoint coordinate of 850 m, where there is no influence of the caustic. Again, ray theory should give an exact result. We see that the pulse obtained by demigration modeling fits again the ray-theoretical pulse very well in amplitude and pulse shape. The amplitude obtained by Kirchhoff modeling is also more or less the same. However, its pulse has suffered some distortion. It is longer than the original source wavelet, and its second leg is not as deep as that of the correct one. The reason is that the plane-wave assumption of the Kirchhoff approximation is violated by the relatively high reflector curvature.

As a final comparison, we address in Figure 6 the amplitudes along the whole seismic sections obtained from the three
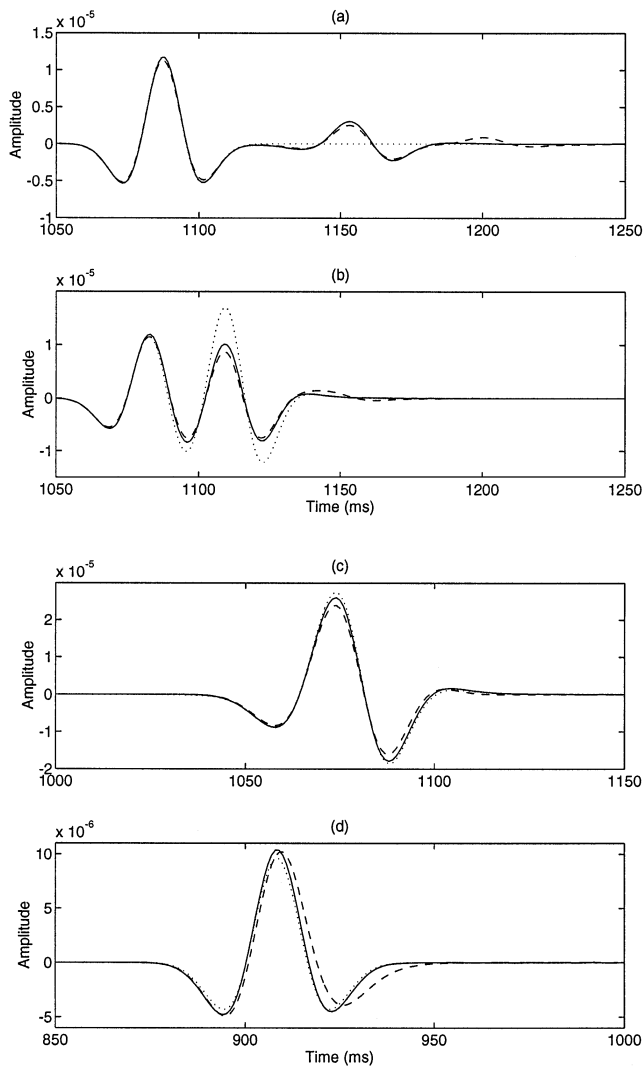


FIG. 5. Comparison of modeling results of zero-order ray theory (dotted line), Kirchhoff modeling (dashed line), and modeling by demigration (solid line). Trace at midpoint (a) 250 m, (b) 340 m, (c) 430 m, and (d) 850 m.
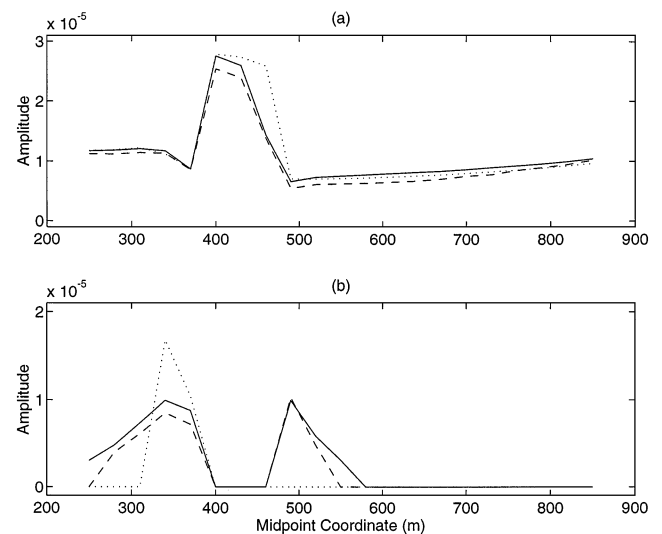


FIG. 6. Comparison of amplitude values along the reflections in Figure 4 as obtained from zero-order ray theory (dotted line), Kirchhoff modeling (dashed line), and modeling by demigration (solid line). (a) First arrival. (b) Second arrival.

different methods. We have picked the peak amplitudes of the two distinguishable events in the three sections. For the amplitudes of the first event (see Figure 6a), modeling by demigration (solid line) reconstructs the same amplitude values as ray theory (dotted line) until a midpoint coordinate of about 400 m. Kirchhoff modeling (dashed line), however, suffers from a certain amplitude loss. Between about 400 and 500 m, ray tracing suffers from incorrect amplitudes because the receiver falls into the caustic region and the two arrivals overlap. Here we see that the amplitudes of modeling by demigration follow more closely the ones obtained from Kirchhoff modeling. Beyond 500 m, all three approximations yield comparable results. Observe that Kirchhoff modeling systematically yields the lowest amplitudes. From the amplitudes of the second event (see Figure 6b), we again observe that modeling by demigration and Kirchhoff modeling provide quite similar results for the diffracted events and the ones close to the caustic. As already indicated, ray theory yields wrong amplitudes in this region. Again, amplitudes from modeling by demigration are slightly greater than those from Kirchhoff modeling.

The slightly lower amplitudes of Kirchoff modeling in comparison to modeling by demigration can be reduced with a smaller sampling interval in the numerical integration. This indicates that the amplitudes obtained by demigration modeling in the example above are indeed better estimates than those from conventional Kirchhoff modeling. For reasons of comparison, however, in this example both integrals were solved numerically using the same sampling interval as well as the same numerical integration technique.

Further numerical examples can be found in an accompanying paper (Santos et al., 2000).

## SUMMARY AND CONCLUSIONS

We have proposed a new seismic forward modeling scheme based on a seismic imaging process called demigration. For a single-reflector example, we have compared the results obtained by the proposed scheme with its counterparts obtained by classical zero-order ray theory and by conventional Kirchhoff forward modeling. For this simple but typical example that includes diffractions, conflicting dips, and even a wavefield caustic, modeling by demigration has apparently provided superior results than the other widely used methods.

In particular, in regions where ray theory is expected to yield good results, modeling by demigration has provided specular reflection pulses that are almost identical to those of ray theory. The modeled wavefield in this region has suffered very little from pulse stretch, phase shifts, or amplitude losses. At the same time, modeling by demigration has accounted for diffractions in a way similar to conventional Kirchhoff modeling. For our simple example, modeling by demigration has combined the advantages of both conventional methods.

Other numerical experiments, not shown in this work, indicate another advantage of modeling by demigration over the other methods: a relatively small sensitivity to nonsmooth reflectors. Even in situations where synthetic data computed by zero-order ray theory or the Kirchhoff forward-modeling integral are severely affected by the lack of smoothness of a reflector, modeling by demigration provided consistently good results.

Moreover, because of its structure, modeling by demigration is especially well suited to perform modeling in time-lapse applications, i.e., to model reservoir changes with time. Since in that case only the artificial migrated section must be changed, the previously computed stacking surfaces and weight functions can be used again without any modifications.

Modeling by demigration links the theory of seismic modeling to that of seismic reflection imaging. Any software developed for true-amplitude Kirchhoff migration can be modified easily to construct synthetic seismograms with the help of true-amplitude modeling by demigration.

## REFERENCES

Berkhout, A. J., 1982, Seismic migration—imaging of acoustic energy by wave field extrapolation: Elsevier.
Beydoun, W. B., and Mendes, M., 1989, Elastic ray-Born $l_2$-migration/inversion: Geophys. J. Roy. Astr. Soc., **97**, 151–160.
Bleistein, N., 1984, Mathematics of wave phenomena: Academic Press Inc.
——— 1987, On the imaging of reflectors in the earth: Geophysics, **52**, 931–942.
Duquet, B., Marfurt, K. J., and Dellinger, J. A., 2000, Kirchhoff modeling, inversion for reflectivity, and subsurface illumination: Geophysics, **65**, 1195–1209, this issue.
Ferber, R. G., 1994, Migration to multiple offsets and velocity analysis: Geophys. Prosp., **42**, 99–112.
Frazer, L. N., and Sen, M. K., 1985, Kirchhoff–Helmholtz reflection seismograms in a laterally inhomogeneous multi-layered elastic medium—**I**. Theory: Geophys. J. Roy. Astr. Soc., **80**, 121–147.
Hubral, P., Schleicher, J., and Tygel, M., 1996, A unified approach to 3-D seismic reflection imaging—Part **I**: Basic concepts: Geophysics, **61**, 742–758.
Jaramillo, H., and Bleistein, N., 1997, Demigration and migration in isotropic inhomogeneous media: 67th Ann. Internat. Mtg., Soc. Expl. Geophys., Expanded Abstracts, 1673–1676.
Kaculini, S., 1994, Time migration and demigration in 3D: Summer workshop, EAEG/SEG, Expanded Abstracts, 66–69.
Nemeth, T., Wu, C., and Schuster, G. T., 1999, Least-squares migration of incomplete reflection data: Geophysics, **64**, 208–221.
Santos, L. T., Schleicher, J., Tygel, M., and Hubral, P., 2000, Seismic modeling, migration, and demigration: The Leading Edge, **19**, scheduled for July.
Schleicher, J., Hubral, P., Tygel, M., and Jaya, M. S., 1997, Minimum apertures and Fresnel zones in migration and demigration: Geophysics, **62**, 183–194.
Schleicher, J., Tygel, M., and Hubral, P., 1993, 3-D true-amplitude finite-offset migration: Geophysics, **58**, 1112–1126.
Sun, J., and Gajewski, D., 1997, True-amplitude common-shot migration revisited: Geophysics, **62**, 1250–1259.
Tygel, M., and Hubral, P., 1987, Transient waves in layered media: Elsevier Science Publ. B.V.
Tygel, M., Schleicher, J., and Hubral, P., 1994a, Kirchhoff–Helmholtz theory in modelling and migration: J. Seis. Expl., **3**, 203–214.
——— 1994b, Pulse distortion in depth migration: Geophysics, **59**, 1561–1569.
——— 1995, Dualities between reflectors and reflection-time surfaces: J. Seis. Expl., **4**, 123–150.
——— 1996, A unified approach to 3-D seismic reflection imaging—Part **II**: Theory: Geophysics, **61**, 759–775.
Whitcombe, D. N., 1991, Fast and accurate model building using demigration and single-step ray-trace migration: 61st Ann. Internat. Mtg., Soc. Expl. Geophys., Expanded Abstracts, 1175–1178.
Whitcombe, D. N., 1994, Fast model building using demigration and single-step ray migration: Geophysics, **59**, 439–449.